Available online at BCREC Website: http://bcrec.undip.ac.id

Bulletin of Chemical Reaction Engineering & Catalysis, 10 (3), 2015, 294-303

Research Article

The Optical Properties and Photo catalytic Activity of ZnS-TiO$_2$/Graphite Under Ultra Violet and Visible Light Radiation

Fitria Rahmawati*), Rini Wulandari, Irvina M. Murni, M. Moedjijono

Research Group of Solid State Chemistry & Catalysis, Chemistry Department, Sebelas Maret University, Jl. Ir. Sutami 36 A Kentingan, Surakarta, Indonesia 57126

Received: 31st May 2015; Revised: 6th August 2015; Accepted: 17th October 2015

Abstract

This paper discuss research about the optical properties and photo catalytic activity of TiO$_2$ film on graphite substrate and its modification with ZnS. The optical properties investigated are the light response at various light wavelength and the gap energy (Eg). Meanwhile, the photocatalytic activity was studied from isopropanol degradation to determine the Quantum Yield (QY) and kinetics of reaction. The results show that the TiO$_2$ layer is consisted of rutile and anatase phases. Meanwhile, the ZnS peaks are at 2θ 27.91° and 54.58°. The gap energy of TiO$_2$/G consist of two band gap representing the band gap of rutile and anatase. The ZnS deposition shifted the band gap into single gap of 3.40 eV which is in between the gap energy of single TiO$_2$ and single ZnS. The isopropanol degradation with TiO$_2$/G photocatalyst under visible light radiation did not produce any new peaks representing product. Meanwhile, the photocatalytic process under 380 nm light produce new peaks representing the electronic transition of acetone. The isopropanol degradation with ZnS-TiO$_2$/Graphite produced new peaks that indicates the photocataytic activity of ZnS-TiO$_2$/Graphite whether under UV or visible light radiation. Significant role of ZnS also proven by the increase of the QY values and the increase of rate constant, k. © 2015 BCREC UNDIP. All rights reserved.

Keywords: ZnS; TiO$_2$; composite; chemical bath deposition; photo catalytic activity

How to Cite: Rahmawati, F., Wulandari, R., Murni, I.M., Moedjijono, M. (2015). The Optical Properties and Photo catalytic Activity of ZnS-TiO$_2$/Graphite Under Ultra Violet and Visible Light Radiation. *Bulletin of Chemical Reaction Engineering & Catalysis*, 10 (3): 294-303. (doi:10.9767/bcrec.10.3.8598.294-303)

Permalink/DOI: http://dx.doi.org/10.9767/bcrec.10.3.8598.294-303

1. Introduction

Modification of TiO$_2$ semiconductor has been conducted by several reseachers [1-3] with the aim to increase the photo catalytic activity of TiO$_2$ especially at visible light radiation. TiO$_2$ is the most studied material for photo catalysis due to its stability, unexpensive, ease of fabrication and produsing a significant voltage [4]. TiO$_2$ also a promising material for photoelectrochemical water splitting in which the water molecules convert to hydrogen fuel and oxygen. The production of solar based fuels might become a very important technology to produce renewable energy. Therefore, to create a stand alone unassisted device that can spontaneously convert solar energy into a chemical bonds of fuels is very important. It must be followed with the improvement of the individual performance of the photocatalyst material [5].

It was found that the coupling of two or

---

*) Corresponding Author
Email: fitria@mipa.uns.ac.id (F. Rahmawati)

more semiconductors decrease the electron-hole recombination [6]. The inhibition of electron-hole recombination might increase the photo catalytic activity of material due to the excited electrons can freely migrate to the semiconductor surface to induce redox reactions. It will produce higher Quantum Yield, QY, than single bulk TiO_2. The QY of hydroxyl radical production by TiO_2 during photocataysis in aqueous solution is $7x10^{-5}$ and the QY of hole generation that was estimated by iodide ion oxidation is $5.7x10^{-2}$ [7]. Meanwhile, the QY of formaldehyde formation with neat colloidal TiO_2 (2.4 nm of particle size) under high energy radiation (351 nm light) is $3.2x10^{-2}$. The value was high, however it was produced by the assistance of laser pulse application. It means that high QY value of TiO_2 could be achieved only by applying some specific treatments. Therefore, some efforts to enhance the photo catalytic activity of TiO_2 are required in order to reach high photo catalytic activity without any specific treatments in the degradation cell.

The low quantum yield of TiO_2 might occur due to the recombination process of the excited electrons in the conduction band with the generated holes in the valence band, before those reducing agents (the excited electrons) and those oxidizing agents (the holes) move to the surface and react with the targeted molecules. Combination with higher band gap semiconductor might be applied to reduce electron-hole recombination. For example, the combination with ZnS with gap energy of 3.8 eV resulting in the enhancement of charge separation in the photocarriers (holes and electrons) generation process occurred at the surface of the anatase TiO2 crystal lattice [8]. The composite of TiO_2/ZnS that was prepared by microemulsion combined with solvo thermal method exhibited a new UV absorption characteristic compared with the bulk TiO_2 or ZnS. The composite also show higher efficiency of visible-light photo catalytic activity to degrade the aqueous parathion methyl compared to pure anatase TiO_2 and ZnS nanoparticle [8]. Meanwhile, the TiO_2/ZnS composite that was prepared by homogeneus hydrolysis of titanium oxo-sulphate and zinc sulphate in aqueous solution with thioacetamide, exhibits better UV characteristic compared to the bulk TiO_2 and ZnS [9]. A homogeneus ZnS coating onto TiO_2 nanoparticle also can be prepared by sonochemical method [10] and also by a microemulsion–mediated solvothermal method that produced an enhanced photocatalytic activity due to strong adsorption of the targeted molecules at the ZnS/TiO_2 nanocomposites surface area [11]. Study on the ZnS doping level into TiO_2 has been conducted at different ratio ZnS:TiO_2 and found that the best catalytic performance on MB photodecolorization was at TiO_2/ZnS 0.2 % which reached the complete photodecolorization 70 mins faster than the TiO_2 photoassisted process [12].

In consideration to eliminate the difficulties and cost reduction on separation process, the immobilized form of photocatalyst might be a better option than a powder form. Some substrate such as titanium foil [13] and also graphite [2,14] have been used. Graphite is a good substrate due to its inert properties, inexpensive and provide high conductivity that allows the application of the semiconductor/graphite as a photoelectrode. In addition, the titania networks can form a strong thin layer on graphite substrate with the assistance of surfactant molecules. A research on combining the carbon based-material with metal oxide semiconductor has also been conducted by combining CdS-graphene/TiO_2 [15]. Graphene is a single layer of graphite that consist of sp2 bonded carbon atoms arranged in a hexagonal lattice. Graphene has high electrical conductivity and has high level light absorption. However, it is still expensive for commercial uses due to high cost production. In addition, to grow a large scale graphene layer requires a metallic substrate and the graphene layer will be damaged when it is separated from the metal subtrate. Therefore, this research prefer to use graphite, due to graphite is a naturally occuring carbon compound that also has a hexagonal lattice structure with high electrical and thermal conductivity, and also very resist of chemical attack. The graphite used in this research is a waste graphite from the zinc-carbon primary battery waste. It is in agreement with environmental friendly production of materials.

2. Materials and Method

All chemicals used were pro analysis grade and procured from Merck, Indonesia. The TiO_2/Graphite was prepared by chemical bath deposition, CBD, based on our previous paper [14]. $TiCl_4$ was used as titania precursor and cetyl trimethyl ammonium bromide was used as linking agent between titania network and graphite substrate. The synthesis solution was prepared in 100 mL of 1 M HCl solution. Deposition was conducted at 60 ^oC for 4 days. The as deposited titania network on graphite substrate then to be annealed at 450 ^oC for 4 hours.

The zinc sulfide precursor solution was prepared by dissolving $ZnSO_4.H_2O$ (0.16 M), ammonia (7.5 M) and thiourea (0.6 M) in deionized water at 80 ^oC [14]. The TiO_2/Graphite was dip into zinc sulfide precursor solution under temperature 80 ^oC in oven. The dipping was conducted for three times, in which each dipping was 15 minutes. The prepared materials were characterized with x-ray diffraction to analyse the presence of specific peaks of targeted elements. Meanwhile, the Scanning Electron Microscopy (JEOL, JED-2300 Analysis Station) analysis was conducted to study the surface morphology, the form of deposited particles and estimate the particle size. The estimation was done by applying MeasureIT software. The elemental analysis of ZnS-TiO_2/Graphite was conducted with EDAX SL Ametex. The elemental composition of TiO_2/Graphite was analyzed by SEM/EDX (JEOL, JED-2300 Analysis Station)

The optical properties of materials i.e light respon at various wavelength, absorption edge and gap energy were studied through UV Vis Diffuse Reflectant spectroscopy (UV 1700 Pharmaspec, Shimadzu, Japan) analysis. Application of Kubelka-Munk equation to the absorbtion data followed by Tauc Plot of direct and indirect transition was used to determine the gap energy values. The Kubelka-Munk equation for direct transition (n=0.5) is written in equation (2) and for indirect transition (n=2) is written in equation (3) [17].

$$F(R'\infty)^2 = \left(\frac{A}{S}\right)^2 (E - E_g) \tag{2}$$

$$F(R'\infty)^{0.5} = \left(\frac{A}{S}\right)^{0.5} (E - E_g) \tag{3}$$

where A is a constant that depends on the properties of the material, E is the energy of photon, E_g is the band gap. S is the dispersion factor, which is independent of the wavelength for particles larger than 5 mm. Sample with opacity greater than 75 % the Kubelka-Munk function, $F(R'\infty)$ might be calculated by equation (4).

$$F(R'\infty) = \frac{(1 - 0.01R)^2}{2(0.01R)} \tag{4}$$

R is the reflection in %.

The photo catalytic activity was determined through isopropanol degradation. Isopropanol was chosen due to this molecule does not photoactive at 200-500 nm. Therefore, the change of absorbance spectrum induced by light radiation represent the actual photo catalytic activity of the photo catalyst without any concern of photo catalytic degradation. The 2.5 M of isopropanol solution was irradiated by 380 nm and 450 nm of light for 30, 60 and 90 minutes. The degradation was conducted in a cuvette with a prepared catalyst tablet that was hang on with a wire. The cuvette was installed in a sample holder of UV Vis spectronic 21 D at the photometric menu. Quantum Yield, Φ, calculated for acetone production was identified at 223-224 nm or 266 nm.

The Quantum Yield calculation was conducted with Equation (5).

$$\Phi = \frac{N_{mol}(mol/s)}{N_{photon}(mol\ Einstein/s)} \tag{5}$$

N_{mol} is the number of isopropanol molecules which was transformed into a product or mol of product formed during photo degradation. $N_{Photons}$ is the number of photon absorbed by the photo catalyst that was determined by UV Vis Diffuse Reflectant spectroscopy. The power of spectroscopy lamp is 50 watt.

3. Results and Discussion

The TiO_2 layer that was deposited by chemical bath deposition on graphite substrate consist of rutile and anatase phases, which are in agreement with standard diffraction of anatase ICSD#9852 and rutile ICSD#23697. Peak of CTAB molecules still presented at 2q 21.3202^o and 24.0444^o. Those are in agreement with CTAB standard diffraction ICSD #110459. The diffraction patterns are described in Figure 1. Meanwhile the ZnS peaks are detected at 2q 27.91^o and 54.58^o. The peaks are stacked with the peaks of rutile at 2θ 27.9187 ^{o} and anatase at 2θ 54.60^o. Le Bail refinement confirmed the presence of ZnS among other phases of rutile, anatase, CTAB and graphite. The Le Bail plot is depicted in Figure 1(b) and the cell parameters arelisted in Table 1. The SEM image (Figure 2 (b)) also confirms the presence of new deposit with flake form, in which the diffraction peaks are in agreement with ZnS standard diffraction ICSD # 15477.

SEM image of TiO_2 layer on graphite shows that the titania dispersed on graphite substrate as spherical form with diameter of 145.9 ± 0.19 nm. Meanwhile, ZnS deposited on TiO_2 as a flake form with diameter of 1.009 ± 0.436 nm. SEM images were depicted in Figure 2. Meanwhile, the elemental analysis by EDX shows the main content is carbon at 51.79 % weight and the Zn content is 35.84 wt.%. EDX analysis also shows the present of Si at 1.48 wt.%, meanwhile the Ti element is only 00.24 wt.%. The EDX spectrum is depicted in Figure 3 (a). The result indicates that the TiO_2 layer might leached out during ZnS deposition. However, the diffraction pattern still confirm the present of TiO_2, eventhough the peak at 2θ 27.9187° and at 2θ 54.60° are coincide with ZnS peaks. In comparison with the EDX spectrum of TiO_2/Graphite, which is described in Figure 3(b). It is known that the peaks at 2.8 keV is actually also a peak of TiK escape. The escape peak occured when the detecting crystal is ionized and emits the X-ray that escape the crystal. The escape peak might present at the energy level lower than the parent peak [18]. The parent peak could be TiKα, which shows the electronic movement from L shell back to K shell, or it might a peak of Ti Kβ which correspond to the electronic movement from M shell to the K shell. Those TiK escape peak seems to be not included in the calculation. In addition, the peaks at 0.45-0.5 keV are also might in coincide with the peak of OKα.

Kubelka-Munk equation that was applied to the diffuse-reflectant data defined the direct transition (n=0.5) and indirect transition (n=2) of each prepared material. Tauc plots were described in Figure 4, that shows the crossing line with x-axis as the gap energy value in electron volt, eV. The gap energies are listed in Table 2. The TiO_2/G shows two gap energies which refer to rutile and anatase phase.

Isopropanol degradation with TiO_2/G at 450 nm light irradiation did not produce new peak as it was produced in degradation at 380 nm of light irradiation (Figure 5). The peaks are at 270 nm that refers to $n\rightarrow\pi^*$ transition of acetone and peak at 221 nm refers to $n\rightarrow\pi^*$ transition of acetone. As it was stated by Kumar [19] that the ketone functional group shows electronic transition at 180 -195 nm for $\pi\rightarrow\pi^*$ and at 270- 295 nm for $n\rightarrow\pi^*$ transition. In a more polar solvent, in which the production of acetonee will increases the polarity of the solvent, the electronic transition of $\pi\rightarrow\pi^*$ might shift to longer wavelength. In this research, the peaks appeared at 221 nm. Its in agreement with the result found by Xu and Raftery that the product of isopropanol degradation is acetone [20].

Meanwhile isopropanol degradation using ZnS-TiO_2/G produced new peaks at 132 nm whether under visible (450 nm) or ultraviolet light (380 nm) radiation (Figure 6). The peaks were shifted to longer wavelength due to high

Table 1. The cell parameters of TiO_2/Graphite and ZnS-TiO_2/Graphite which was refined with the specific crystal structure.

	TiO_2/Graphite		ZnS-TiO_2/Graphite		
Cell parameters	Rutil	Anatase	Rutil	Anatase	ZnS
Crystal structure	Tetragonal	Tetragonal	Tetragonal	Tetragonal	Hexagonal
Space group	*P42/mnm*	*I41/amd*	*P42/mnm*	*I41/amd*	*P63MC*
a (Å)	4.3428	3.684(2)	4.60(2)	3.7842	3.8293(6)
b (Å)	4.3428	3.684(2)	4.60(2)	3.7842	3.8293(6)
c (Å)	2.8912	9.5146	2.9589	9.5146	31.200003
angle	$\alpha=\beta=\gamma=90^\circ$	$\alpha=\beta=\gamma=90^\circ$	$\alpha=\beta=\gamma=90^\circ$	$\alpha=\beta=\gamma=90^\circ$	$\alpha=\beta= 90^\circ$ $\gamma=120^\circ$
Cell volume (Å^3)	54.527782	129.14(8)	62.6(3)	136.250687	396.20(9)
Rp (%)	4.655		2.123		
Rwp (%)	6.365		3.692		

Table 2. The gap energy of the prepared materials, n=0.5 is direct band gap and n=2 is indirect band gap.

Materials	Eg(n=0.5) (eV)	Eg(n=2) (eV)
TiO_2 P25-Degussa/Graphite	3.16	3.50
TiO_2/Graphite	3.02	3.43
	3.02	3.20
ZnS-TiO_2/Graphite	3.16	3.40

polarity of solution in the degradation cell. It also indicates the strong interaction between the isopropanol molecules and the molecules as degradation result with the ZnS-TiO_2/Graphite composite. The strong interaction might be a form of preassociated complex between molecules and the composite [11]. FTIR analysis on the isopropanol solution before and after photocatalytic degradation with ZnS-TiO_2/G shows disappearance of some specific peaks, i.e peak of OH strectching at 3419 cm^{-1}, CH Aliphatic at 2922 cm^{-1}, OH bending at 1697 cm^{-1} and CH bending at 1398 cm^{-1}. The FTIR spectrum is depicted in Figure 7.

The quantum yield calculation found that ZnS-TiO_2/G has higher photocatalytic activity at visible light than at ultraviolet light. Based on the gap energy of ZnS-TiO_2/G, i.e. 3.40 eV, the catalyst will photoactive under wavelength light of 364.9 nm or shorter. However, the isopropanol and QY calculation shows that the composite has higher activity under visible light radiation. Its may indicates the contribution of graphite substrate on light adsorption. As it was confirmed by UV-Vis diffused-reflectance of the composite that shows the $\pi \rightarrow \pi^*$ transition of graphite (Figure 4(a)). Its in agreement with the contribution of graphene, as another form of a carbonaceous molecules, which also can increase the photo-

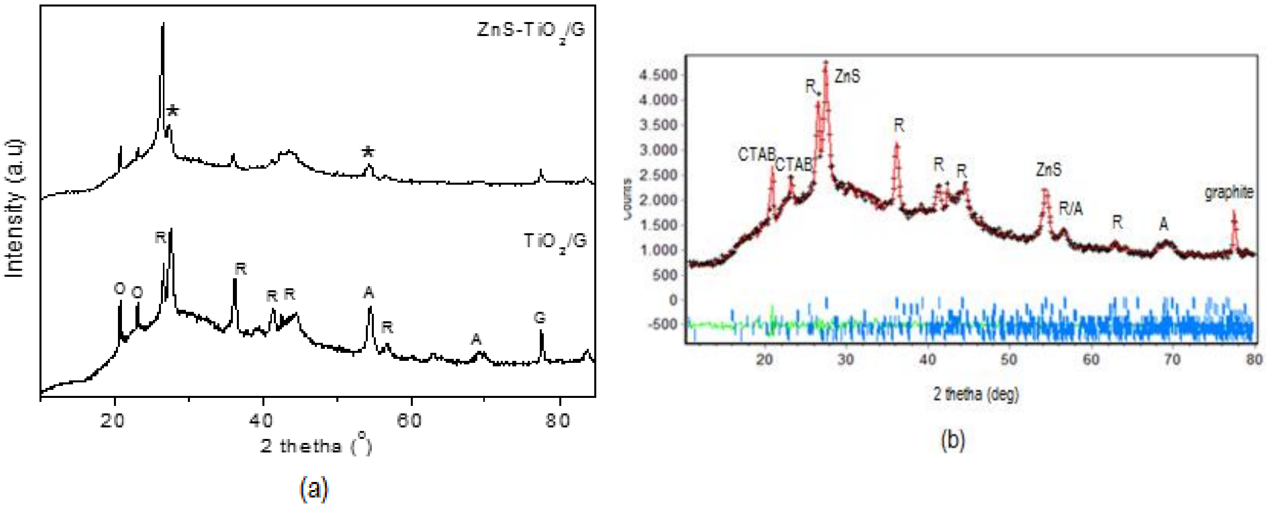

(a) (b)

Figure 1. (a) The diffraction patterns of TiO_2/G and ZnS-TiO_2/G. R refers to rutile phase, A refers to anatase, G refers to Graphite, O refers to CTAB and * refers to ZnS peak in agreement with ZnS standard ICSD # 15477; and (b) The Le Bail plot of ZnS-TiO_2/Graphite.

Table 3. The Quantum Yield and N_{photon} (mol.s^{-1}) of TiO_2/G and ZnS-TiO_2/G under 450 nm and 380 nm radiation.

Light source (nm)	Materials	N_{photon} (mol.s^{-1})	Quantum Yield
450	TiO_2/G	$1.11x10^{-5}$	0
	ZnS-TiO_2/G	$1.85x10^{-4}$	$6.00x10^{-2}$
380	TiO_2/G	$6.58x10^{-3}$	$1.96x10^{-3}$
	ZnS-TiO_2/G	$5.87x10^{-3}$	$7.30x10^{-3}$

Table 4. The rate constants and linearity coefficients of the isopropanol degradation with TiO_2/Graphite and ZnS-TiO_2/Graphite.

Materials	Wavelength of photon source (nm)	Rate constant (min^{-1})	Linearity coefficient
TiO_2/G	450	0	0
	380	$1.60x10^{-3}$	0.99
ZnS-TiO_2/G	450	$1.45x10^{-1}$	0.91
	380	$3.29x10^{-2}$	1.00

absorption effect [15]. The increasing of photocatalytic activity by the presence of ZnS might also be attributed to the formation of preassociated complex between ZnS/TiO_2 composite with isopropanol molecules, the synergetic effect of ZnS and TiO_2, and strong absorption between isopropanol molecules and ZnS/TiO_2 composite [11]. The visible light photoactivity was also founded in the nanocomposite of TiO_2/ZnS that was synthesized by homogeneus hydrolysis in aqueous solution with thioacetamide in the degradation of orange II dye solution [3]. Although, its band gap energy is high, however the activity at visible light indicates that actually if UV light provides the photons

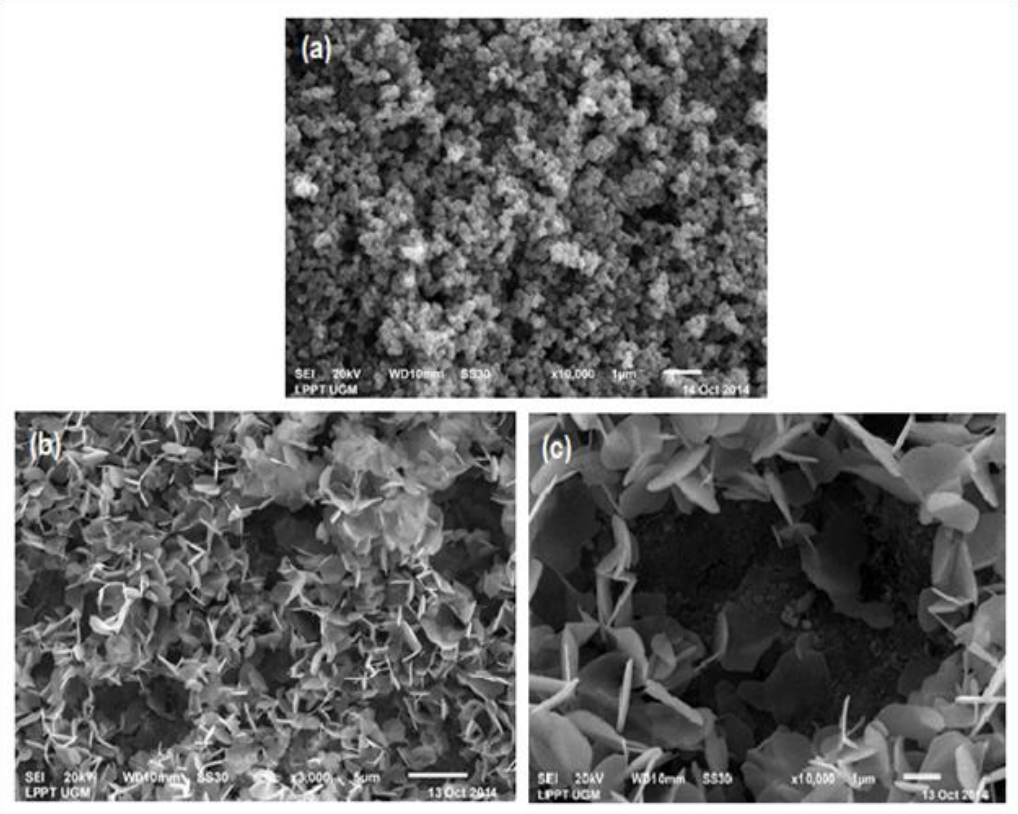

Figure 2. SEM images of (a) TiO_2/Grafit and (b), (c) ZnS-TiO_2/Grafit at different magnification

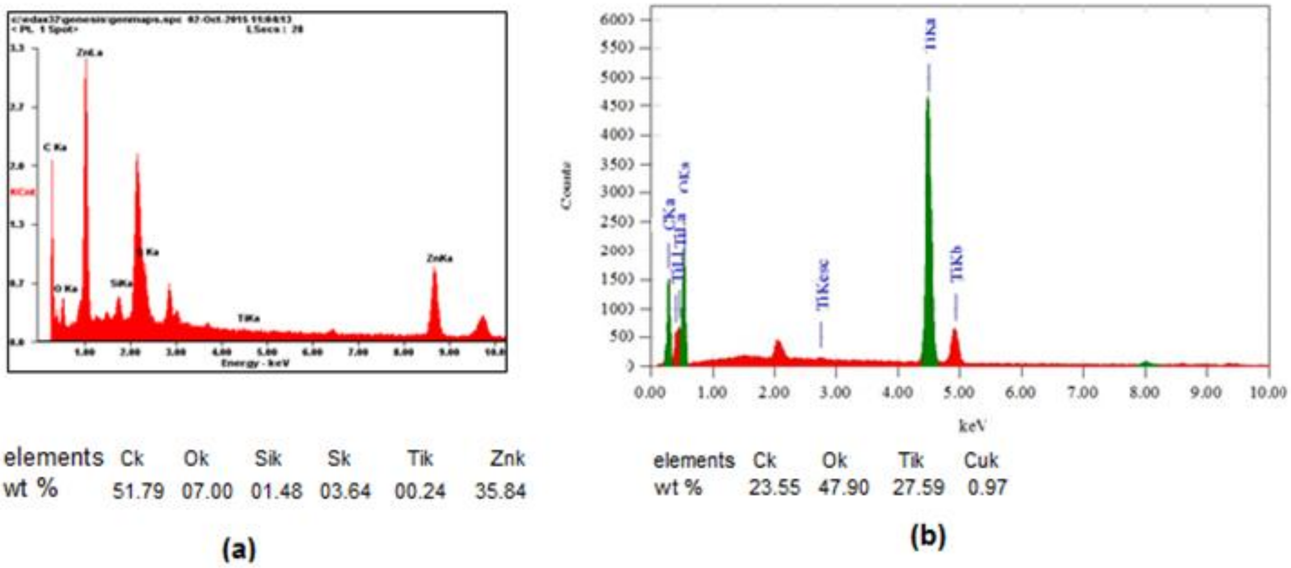

elements	Ck	Ok	Sik	Sk	Tik	Znk
wt %	51.79	07.00	01.48	03.64	00.24	35.84

(a)

elements	Ck	Ok	Tik	Cuk
wt %	23.55	47.90	27.59	0.97

(b)

Figure 3. The EDX spectrum of ZnS-TiO_2/Graphite and its composition (a) and the EDX spectrum of TiO_2/Graphite and its composition (b)

required for the electron transfer from valence band to conduction band. Therefore, the energy of of photon is related to wavelength, Meanwhile, the overal energy input to a photocatalytic process is dependent upon the light intensity [3]. It is supported by the data of the number of photon absorbed by ZnS-TiO_2/Graphite per second (Table 3) that increased one order after ZnS deposition. It means that with the same wavelength and

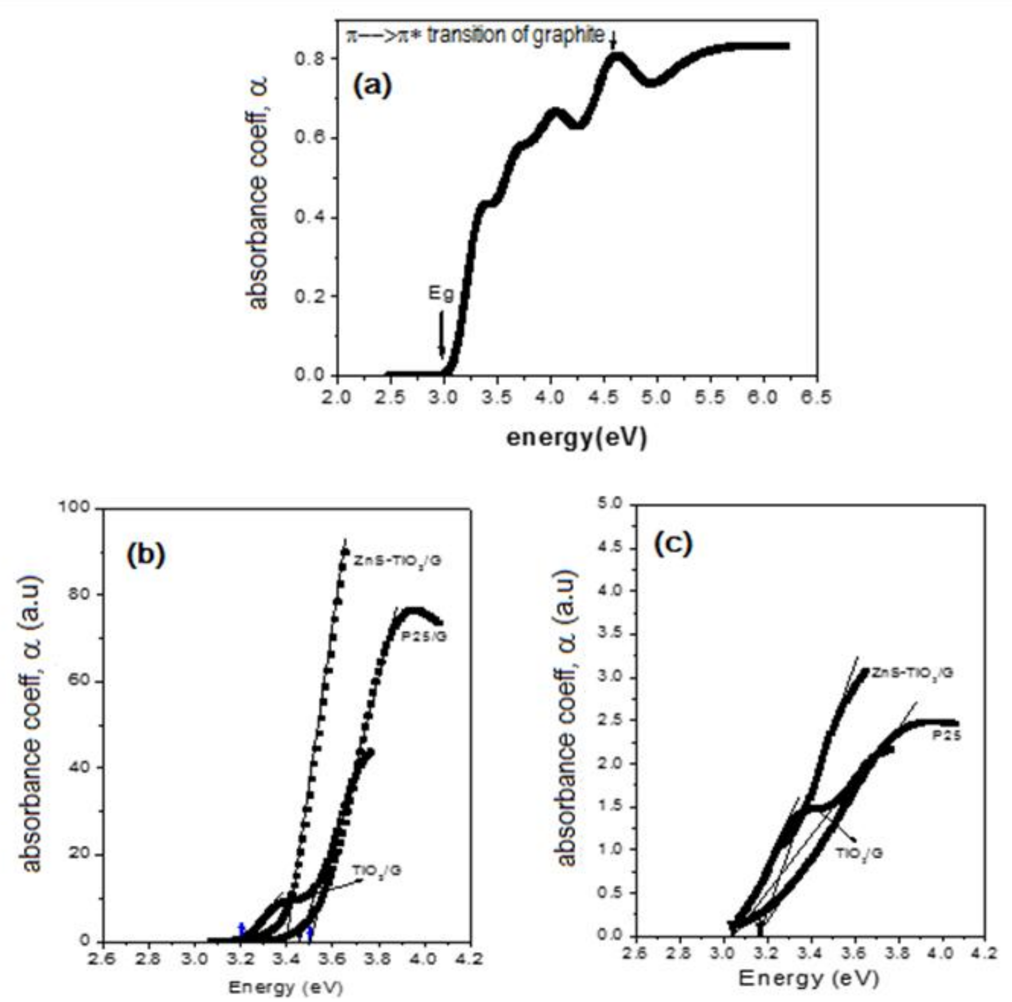

Figure 4. The Tauc plot of (a) TiO_2/Graphite [17], (b) direct transition and (c) indirect transition of the prepared materials

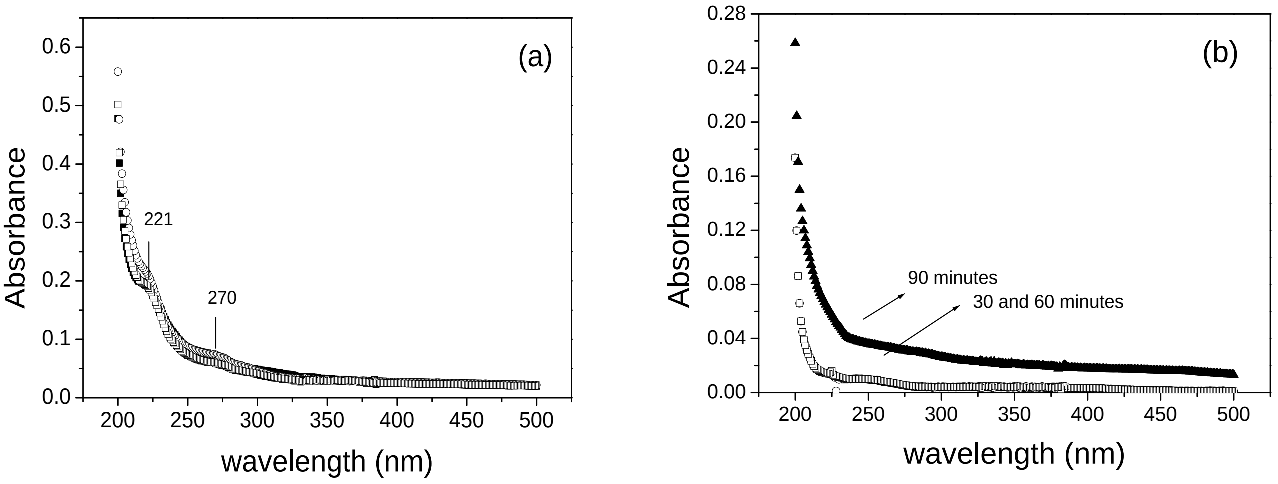

Figure 5. Isopropanol degradation with TiO_2 at (a) 380 nm and (b) 450 nm

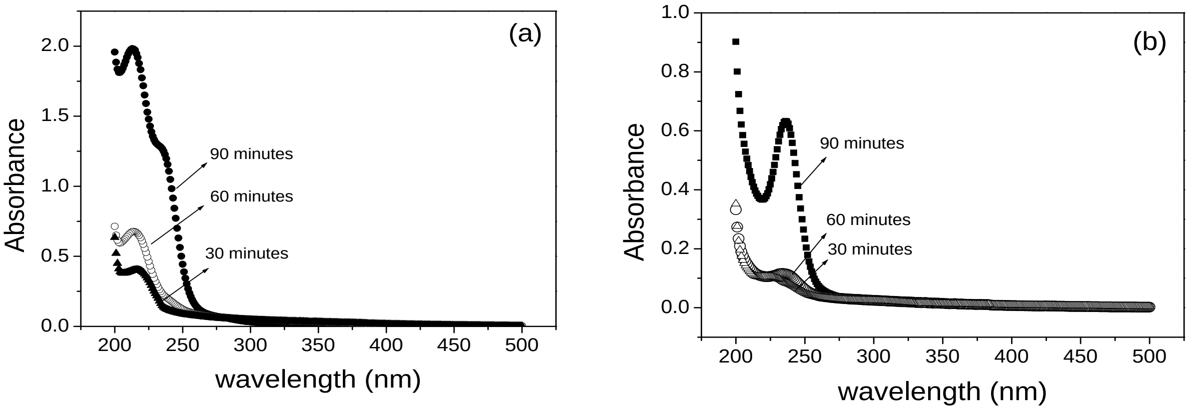

Figure 6. Isopropanol degradation with ZnS-TiO_2 at (a) 380 nm and (b) 450 nm

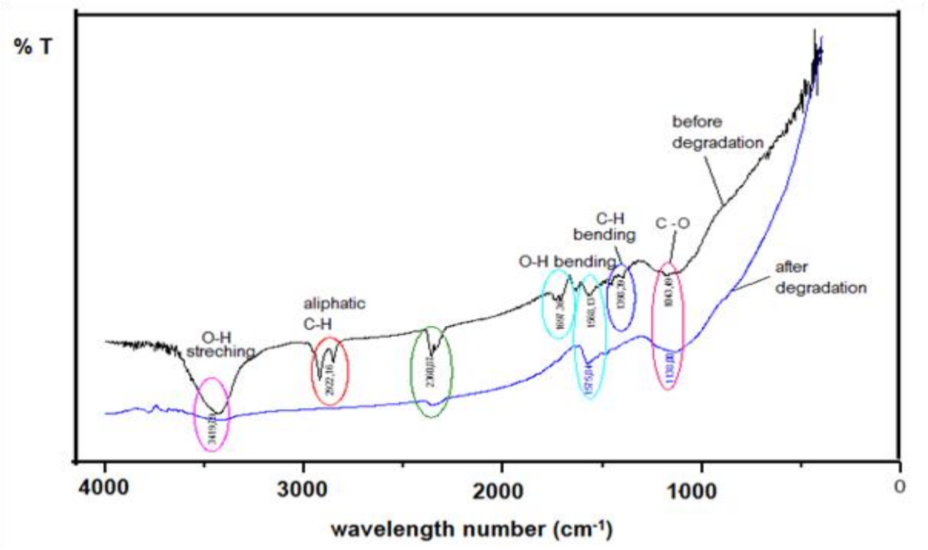

Figure 7. FTIR spectrum of isopropanol solution before and after photocatalytic degradation with ZnS-TiO_2/Graphite.

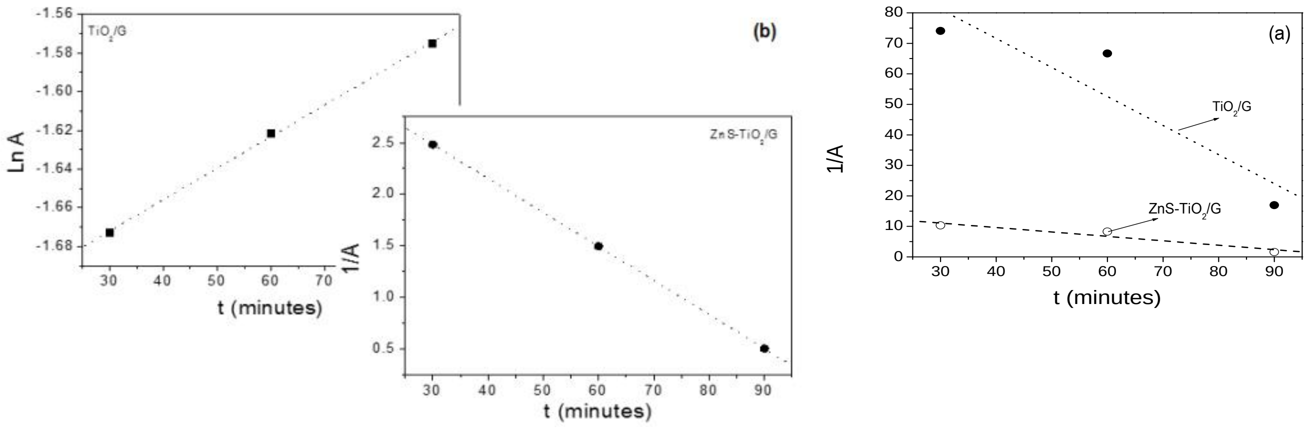

Figure 8. The Kinetic Plots of isopropanol degradation with TiO_2/G and ZnS-TiO_2/G as photocatalyst under irradiation of (a) 450 nm and (b) 380 nm light.

intensity of light, the ZnS-TiO_2/Graphite composite absorbed more photons than TiO_2/Graphite.

The kinetics study found that the isopropanol degradation under 450 nm of light radiation follows second order reaction with the rate constants as listed in Table 4. Meanwhile, the isopropanol degradation under radiation of 380 nm light with TiO_2/G as photocatalyst follows first order and degradation with ZnS-TiO_2/G follows second order reaction. The kinetic plots are described in Figure 7. The rate constant increased from $1.6x10^{-3}$ to $3.29x10^{-2}$ (Table 4). It indicates that ZnS played significant role in the photocatalytic activity. The contribution of ZnS is increasing photon absorbed when the composite was used under visible light. The photon absorbed was increase from $1.11x10^{-5}$ mol.s^{-1} to $1.85x10^{-4}$ mol.s^{-1}. Meanwhile, under UV light radiation, eventhough the photon absorbed by ZnS-TiO_2/G was lower than that was absorbed by TiO_2/G (Table 2), however the QY value is higher than TiO_2/G. It indicates that, the ZnS can serve as the electrons sink of the excited electrons in the conduction band of TiO_2. The charge transfer process may inhibites the possibility of electron-hole recombination.

4. Conclusion

ZnS deposition on TiO_2/Graphite allows increasing of band gap energy. However, it provide the photon absorption increasing under visible radiation, then it become active with QY value of $6x10^{-2}$. Meanwhile, under UV irradiation, the photon absorption of ZnS-TiO_2/G is lower than TiO_2/G, however the QY value increases from $1.96x10^{-3}$ to $7.30x10^{-3}$. It represents the contribution of ZnS to reduce the possibility of electron-hole recombination.

Acknowledgement

This research is part of Hibah Mandatory 2015 funded by PNBP Sebelas Maret University. Authors thank to the financial support.

References

[1] Wang, X.F., Zhang, W. (2014). Chemical depositing of CdS/ZnS composition nanostructure modified TiO_2 thin film. *Chalcogenide Letters*, 11(8): 389-395.

[2] Rahmawati, F., Wahyuningsih, S., Irianti, D. (2014). The Photo catalytic Activity of SiO2-TiO2/Graphite and Its Composite with Silver and Silver Oxide. *Bulletin of Chemical Reaction Engineering & Catalys*is, 9 (1): 45-52.

[3] Stengl, V., Bakrdjieva, S., Murafa, N., Houskova, V., Lang, K. (2008). Visible light photocatalytic activity of TiO2/ZnS nanocomposites prepared by homogeneous hydrolysis. *Microporous and Mesoporous Materials*, 110: 370-378.

[4] Hwang, Y.J., Hahn, C., Liu, B., Yang, P. (2012). Photoelectrochemical properties of TiO2 nanowire arrays: a study of the dependence on length and atomic layer deposition coating. *ACS Nano*, 6: 5060-5069.

[5] Kim, D., Sakimoto, K.K., Hong, D., Yang, P. (2015). Artificial photosynthesis for sustainable fuel and chemical production, *Angewante Chemistry International Edition*, 54: 2-10.

[6] Tambwekar, S.V., Venugopal, D., Subrahmanyam, M. (1999). H_2 production of (CdS-ZnS)-TiO_2 supported photocatalytic system. *International Journal of Hydrogen Energy*, 24 : 957-963.

[7] Ishibashi, K., Fujishima, A., Watanabe, T., Hashimoto, K. (2000). Quantum yields of active oxidative species formed on TiO2 photocatalyst. *Journal of Photochemistry and Photobiology A: Chemistry*, 134: 139-142.

[8] Xiaodan, Y., Qingyin, W., Shicheng, J., Yihang, G. (2006). Nanoscale ZnS/TiO_2 composites: preparation, characterization, and visible-light photocatalytic activity. *Material Characterization*, 57: 333-341.

[9] Stengl,V., Bakardjieva, S., Murafa, N., Houskova, V., Lang, K. (2008). Visible light photocatalytic activity of TiO_2/ZnS nanocomposite prepared by homogeneous hydrolysis. *Microporous and Mesoporous Materials*, 110 : 370-378.

[10] Lee, S.S., Byun, K-T., Park, J.P., Kim, S.K., Lee, J.Ch., Chang, S-K., Kwak, H.-Y., Shim, I-W.(2008). Homogeneous ZnS-coating onto TiO2 nanoparticles by a simple one pot sonochemical method. *Chemical Engineering Journal*, 139: 194-197.

[11] Xiaodan, Y.,Qingyin, W., Shicheng, J., Yihang, G. (2006). Nanoscale ZnS/TiO_2 composites: preparation, characterization, and visibe-light photocatalytic activity. *Material Characterization*, 57: 333-341.

[12] Franco, A., Neves, M.C., Ribeiro Carrott, M.M.L., Mendon, M.H., Pereira, M.I., Monteiro, O.C. (2009). Photocatalytic decolorization of methylene blue in the presence of TiO_2/ZnS nanocomposites. *Journal of Hazardous Mate*rials, 161: 545-550.

[13] Weizhen, H., Park, S-.J., Shin, D-.H., Yoon, S-.J., Wu, Y., Qiu, J., Hwang, Y-.H., Kim, H-.K., Kim, B. (2011). Effect of Annealing Ti Foil on The Structural Properties of Anodic TiO_2

Nanotube Arrays. *Journal of the Korean Physical Society*, 58(3): 575-579.

[14] Rahmawati, F., Kusumaningsih, T., Hapsari, A.M., Hastuti, A. (2010). Ag and Cu loaded on TiO_2/graphite as a catalyst for E. Coli-contaminated water disinfection. *Chemical Papers*, 64: 557-565.

[15] Park, Y., Kefayat, U., Vikram , N., Ghosh, T., Oh, W.C., Cho, K.Y. (2014). Preparation of novel CdS-graphene/TiO_2 composites with high photocatalytic activity for methylene blue dye under visible light. *Bulletin of Material Science*, 36(5): 869-876.

[16] Nakada, T., Masashi, H., Hayashi, E. (2003). Band offset of high efficiency CBD-ZnS CIGS thin film solar cells. *Thin Solid Films*, 431-432: 242-248.

[17] Valencia, S., Marín, J.M., Restrepo, G. (2010). Study of the Band Gap of Synthesized Titanium Dioxide Nanoparticules Using the Sol-Gel Method and a Hydrothermal Treatment. *The Open Material Science Journal*, 4: 9-14

[18] Hafner, B. (14 October 2015) Energy Dispersive Spectroscopy on the SEM: a primer. Citing internet sources http://www.charfac.umn.edu/instruments/eds_on_sem_primer.pdf

[19] Rahmawati, F., Wulandari, R., Murni, I.M., Mudjijono. (2015). Optical properties and photo catalytic activity of CdS-TiO_2/Graphite composite. *Ahead o Print in Science and Engineering of Composite Materials*. DOI: 10.1515/secm-2015-0162

[20] Kumar, S. (2006). *Organic Chemistry: Spectroscopy of organic compounds*, Department of Chemistry, Guru Nanak Dev University, Amritsar, pp. 1-36.

[21] Xu, W., Raftery, D. (2001). Photocatalytic Oxidation of 2-Propanol on TiO_2 Powder and TiO_2 Monolayer Catalysts Studied by Solid-State NMR. *Journal of Physical Chemistry B*, 105: 4343-4349.